Information of Electromagnetic Scattering and Radiative Transfer in Natural Media

Ya-Qiu Jin

Science Press ,Beijing

Information of Electromagnetic Scattering and Radiative Transfer in Natural Media

Ya-Qiu Jin

Science Press, Beijing

Responsible Editors: Bin PENG and Guoying QIN
Cover Designer : Haiying GAO

Published by Science Press
16 Donghuangchenggen North Street
Beijing, 100717
P. R. China

Printed in Beijing

ISBN 7-03-008259-1

Dr. Ya-Qiu Jin graduated from Peking University, China in 1970. He received M.S., E.E., and Ph.D. degrees from the Department of Electrical Engineering and Computer Sciences, the Massachusetts Institute of Technology, USA in 1982, 1983 and 1985, respectively.He held the UK Royal Society Fellowship in 1993 and the Senior Research Associateship of the USA National Research Council in 1996. He is now a Professor in the Department of Electronic Engineering and Director of the Center for Wave Scattering and Remote Sensing, Fudan University, Shanghai, China. He is the Chairman of IEEE GISS Beijing Chapter and the Fellow of CIE.

Introduction

This book collected some journal papers published by the author with his collaborators during 1980-1999, whilst he was a graduate student for Ph.D. degree in the Massachusetts Institute of Technology, USA and till now he holds professorship in the Fudan University, China.

This book summarizes the contributions by the author with his collaborators on the areas such as electromagnetic wave scattering, propagation in random media, modeling and simulation for quantitative microwave remote sensing, data validation and parameters retrieval from measurements of satellite-borne remote sensing, and computational electromagnetics of complex media. It contains six parts. Each part is focus on one topic. The first part discusses the vector radiative transfer (VRT) theory for the study of multiple scattering and radiative transfer of polarized electromagnetic intensity - Stokes vector. The VRT theory for modeling of natural media, such as atmospheric precipitation, sea ice, vegetation canopy and land surfaces, and numerical simulation for space-borne microwave remote sensing are developed. The VRT theory for strongly fluctuating, anisotropic random media, and high-dimensional VRT equation are also discussed in this part.

Advance of polarimetric measurement and imagery of SAR technology has greatly promoted study of fully polarimetric scattering of the Earth surfaces. Part 2 presents simulation of the Mueller matrix solution for multi-layered, multi-components, and non-uniformly oriented, nonspherical scatterers for modeling canopy surfaces. The theory of coherency matrix, eigenvalues and entropy are developed, and are compared with SAR images.

Part 3 discusses scattering from randomly rough surface. High-order scattering from rough surface and shadowing function are discussed. Angular enhancement of backscattering is analytically derived. To model sea surface driven by strong winds, a composite model of foam scatterers with two-scale surface approximation is developed, and is applied to active and passive remote sensing of sea surface winds.

Part 4 is, especially, devoted to strong fluctuation theory. Scattering coherency from strongly fluctuating media, and dense scatterers are studied. It is an important progress to conventional VRT where independent scattering is usually assumed. This theory is applied to remote sensing of snow fields. The VRT equation with multiple scattering for strongly fluctuating random media is refereed to Part 1.

Part 5 contains a lot of simulation, data validation and parameter retrieval from satellite-borne remote sensing, such as DMSP SSM/I. Theoretical simulation, measurements and data from remote sensing observation are linked to quantitatively invert information for the Earth surfaces, e.g. vegetation canopy, snow, sea ice, sea surface winds, sand, flooding, etc., and spatial and temporal variations. Correlation of active and passive remote sensing is demonstrated. Some novel retrieval algorithms such as meshed graph, ANN(artificial neural network) method, statistics of spatial auto-correlation etc. are presented. A novel system of combined scatterometer and radiometer at X band and fields experiments are introduced.

Part 6 discusses computational electromagnetics of complex media. For example, the

T-matrix solution for collective scattering of clustered non- spherical scatterers , the effective dielectric property of particulate media, electromagnetuics of chiral media and dyadic Green's function, the broadened width of angular correlation function on non-memorial line to detect a target situated over rough surface, the fast multi-pole method of the 3D volume integral equation are discussed.

The author greatly appreciates the support from the Divisions of the Earth Science and Information Science of the National Natural Science Foundation of China during his research works at the Fudan University. He is very grateful to his advisors, collaborators and students for their contributions.

Contents

Part I

Theory of Vector Radiative Transfer in Random Media for Remote Sensing Modeling

Passive and Active Remote Sensing of Atmospheric Precipitation *

Y. -Q. Jin , J. A. Kong

Both passive and active remote sensing of atmospheric precipitation are studied with the vector radiative transfer equations by making use of the Mie scattering phase functions and incorporating the raindrop-size distributions. For passive remote sensing we employ the Gaussian quadrature method to solve for the brightness temperatures. For active remote sensing an iterative approach carrying out to the second order in albedo is used to calculate for the bistatic scattering coefficients, the backscattering cross sections/unit volume, and the interchannel cross talks. The calculated results are plotted as a function of rainfall rates and compared to various available experimental data. The theoretical model is easily applied to the remote sensing of aerosol particles, smoke, fog, and haze at infrared and visible frequencies.

I. Introduction

Electromagnetic wave scattering at visible, infrared, and microwave frequencies by a turbid atmosphere (precipitation, cloud, smoke, haze, fog, etc.) was studied extensively for both passive and active remote sensing.[1-6] The scatterers are generally modeled as spherical Mie scatterers, and the radiative transfer (RT) equations are applied. In passive probing of rain rates the scalar RT theory has been used.[3,4] In active remote sensing of the atmosphere the single-scattering assumption is often used.[7] In scalar RT approaches the assumed Gaussian phase function[6] is proposed, which is based on small angle approximation.

In this paper we apply the vector radiative transfer equation to study both the passive and active remote-sensing problems. The Mie scattering phase function matrix is used and averaged over the raindrop-size distributions to solve for the brightness temperatures and the scattering coefficients. We use the Gaussian quadrature method to solve for the brightness temperatures in passive remote sensing. In active remote sensing all four Stokes parameters (I_v, I_h, U, V) are employed. Every term of the phase function matrix is expressed as a truncated series. We use the iterative approach to the second order in albedo to calculate for the backscattering cross section, bistatic scattering coefficients, and interchannel cross talk.[8] Both the passive and active remote-sensing results are compared with experimental data. The same technique can be applied to the remote probing of atmospheric aerosol, cloud, smoke, haze, and fog at infrared or optical frequencies.

II. Theory for Passive Remote Sensing

Consider a precipitation layer consisting of spherical raindrops with permittivity ε_s, which is calculated by the Debye formula.[10] The layer consists of a distribution of different drop sizes and extends from $z = 0$ to $z = -d$ (Fig. 1). Medium 2 is assumed homogeneous. The radiative transfer equations inside the rain layer take the following forms:

$$\cos\theta \frac{d}{dz}\begin{bmatrix} I_v(\theta,z) \\ I_h(\theta,z) \end{bmatrix} = (\kappa_{ad} + \kappa_{ag})CT_1 - (\kappa_{ed} + \kappa_{ag})\begin{bmatrix} I_v(\theta,z) \\ I_h(\theta,z) \end{bmatrix} + \int_0^{\pi} d\theta' \sin\theta' \begin{bmatrix} (v,v') & (v,h') \\ (h,v') & (h,h') \end{bmatrix}\begin{bmatrix} I_v(\theta',z) \\ I_h(\theta',z) \end{bmatrix}, \quad (1)$$

where $I_v(\theta,z)$ and $I_h(\theta,z)$ are the specific intensities for the vertical and horizontal polarizations, T_1 is the temperature of the raindrops and the atmosphere, $C = K/\lambda^2$ with K denoting the Boltzmann constant and λ the free-space wavelength, $\kappa_{ed} = \kappa_{sd} + \kappa_{ad}$ is the extinction coefficient of raindrops, κ_{sd} and κ_{ad} are the scattering and absorption coefficients, κ_{ag} is the absorption coefficient of atmospheric gases (water vapor and oxygen), $0 < \theta < \pi$, and (v,v'), (v,h'), (h,v'), and (h,h') are the Mie scattering phase functions.[1]

We assume an ocean or land background with temperature T_2. The boundary conditions are, for $0 < \theta < \pi/2$, at $z = 0$

* This paper was published in *Applied Optics*, 1983, **22**(17):2535-2545.

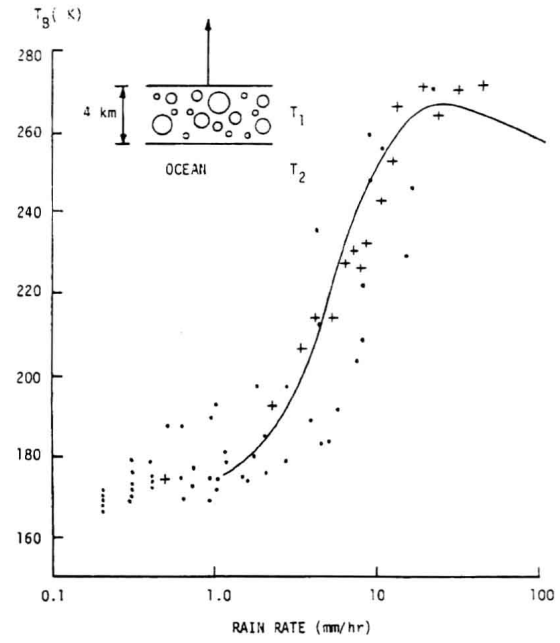

Fig. 1. Geometrical configuration of the problem.

$$\begin{bmatrix} I_v(\pi-\theta,0) \\ I_h(\pi-\theta,0) \end{bmatrix} = 0 \tag{2}$$

and at $z = -d$

$$\begin{bmatrix} I_v(\theta,-d) \\ I_h(\theta,-d) \end{bmatrix} = \begin{bmatrix} r_v(\theta) I_v(\pi-\theta,-d) \\ r_h(\theta) I_h(\pi-\theta,-d) \end{bmatrix} + CT_2 \begin{bmatrix} 1-r_v(\theta) \\ 1-r_h(\theta) \end{bmatrix}, \tag{3}$$

where $r_v(\theta)$ and $r_h(\theta)$ are, respectively, the reflectivities for the vertical and horizontal polarizations.[2]

The brightness temperatures as measured by radiometers are simply

$$\begin{bmatrix} T_{Bv} \\ T_{Bh} \end{bmatrix} = \frac{1}{C} \begin{bmatrix} I_v(\theta,0) \\ I_h(\theta,0) \end{bmatrix} \tag{4}$$

at $z = 0$ and

$$\begin{bmatrix} T_{Bv} \\ T_{Bh} \end{bmatrix} = \frac{1}{C} \begin{bmatrix} I_v(\pi-\theta,-d) \\ I_h(\pi-\theta,-d) \end{bmatrix} \tag{5}$$

at $z = -d$. The task is to solve the radiative transfer Eqs. (1) subject to the boundary conditions (2) and (3).

Numerical solutions are facilitated by replacing the integral in Eq. (1) by Gaussian quadratures[1,7]:

$$\mu_i \frac{d}{dz} \begin{bmatrix} I_v(\theta_i,z) \\ I_h(\theta_i,z) \end{bmatrix} = (\kappa_{ad} + \kappa_{ag}) C T_1 - (\kappa_{ed} + \kappa_{ag}) \begin{bmatrix} I_v(\theta_i,z) \\ I_h(\theta_i,z) \end{bmatrix} + \sum_{j=-N}^{N} a_j \begin{bmatrix} (v_i,v_j)\ (v_i,h_j) \\ (h_i,v_j)\ (h_i,h_j) \end{bmatrix} \begin{bmatrix} I_v(\theta_j,z) \\ I_h(\theta_j,z) \end{bmatrix}, \tag{6}$$

where $i = \pm 1, \ldots, \pm N$, $\mu_i = \cos\theta_i$, and a_j are the Christoffel numbers. In our calculation we use $N = 6$.

In Figs. 2 and 3 we illustrate the brightness temperatures calculated for an ocean background for a precipitation layer with 4-km thickness. The Marshall-Palmer distribution is used to average over the raindrop-size distributions. We see that both T_{Bv} and T_{Bh} are cold at a small rain rate due to the cold ocean background. As the rain rate increases, the brightness

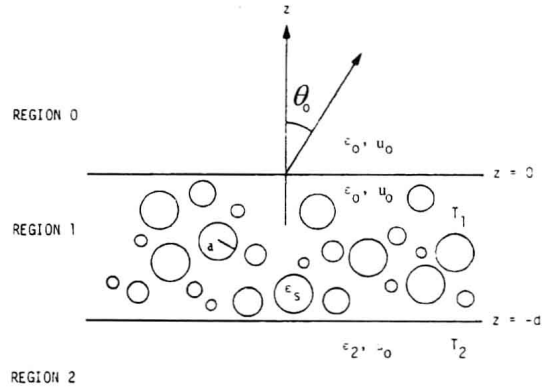

Fig. 2. Brightness temperature vs rain rate at 19.35 GHz. Data given in Ref. 3.

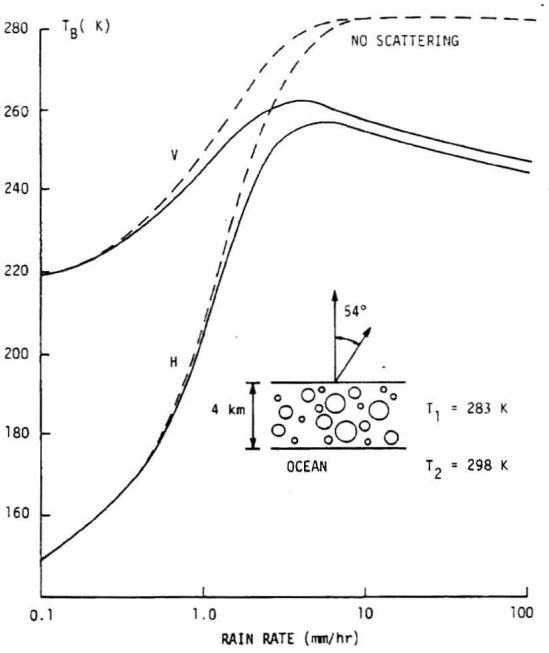

Fig. 3. Brightness temperature vs rain rate at 37 GHz.

temperature increases due to emission from the raindrops. However, compared with the calculation without taking into account the Mie scattering effects as shown with dashed lines, the scattering induces darkening effects, especially at higher rain rates. In Fig. 2 we show that the rainfall model calculations are in good agreement with data collected by Wilheit *et al.*[3] Dots are from simultaneous measurements of the brightness temperatures over ocean by the Nimbus 5 ESMR and the rain rates by the WSR-57 meteorological radar. Crosses are inferred from ground-based measurements of the brightness temperatures and direct measurements of rainfall rates.

III. Theory for Active Remote Sensing

The atmospheric precipitation is modeled as a layer of spherical Mie scatterers with permittivity ε_s and radius a governed by the Laws-Parson distribution, which has been used in most studies of active probing of

rainfall. For active remote sensing the vector radiative transfer equation takes the form[1]

$$\cos\theta \frac{d}{dz}\bar{I}(\theta,\phi,z) = -\kappa_a \bar{I}(\theta,\phi,z) - \kappa_s \bar{I}(\theta,\phi,z) + \int_0^{\pi} d\theta' \sin\theta' \int_0^{2\pi} d\phi' \bar{\bar{P}}(\theta,\phi;\theta',\phi')\, \bar{I}(\theta',\phi',z), \tag{7}$$

where the specific intensity $\bar{I}$ contains all four Stokes parameters

$$\bar{I}(\theta,\phi,z) = \begin{bmatrix} I_v(\theta,\phi,z) \\ I_h(\theta,\phi,z) \\ U(\theta,\phi,z) \\ V(\theta,\phi,z) \end{bmatrix}. \tag{8}$$

$\bar{\bar{P}}(\theta,\phi;\theta',\phi')$ is the scattering phase-function matrix, and κ_a and κ_s are the absorption and scattering coefficients calculated by the Mie theory incorporating the Laws-Parsons size distribution for atmospheric precipitations.

For a plane wave propagating in the direction θ_{oi},ϕ_{oi} and impinging on a precipitation layer of thickness d we write the boundary conditions at $z = 0$ and $z = -d$ as, for $0 < \theta < \pi/2$,

$$\bar{I}(\pi - \theta,\phi,z = 0) = \bar{I}_{oi}\delta(\cos\theta - \cos\theta_{oi})\delta(\phi - \phi_{oi}), \tag{9a}$$

$$\bar{I}(\theta,\phi,z = -d) = 0. \tag{9b}$$

The bistatic scattering coefficient is defined as the ratio of scatterer power of polarization β/unit solid angle in the direction of θ_s and ϕ_s to the incident power of polarization in the direction θ_{oi} and ϕ_{oi} averaged over 4π rad:

$$\gamma_{\beta\alpha}(\theta_s,\phi_s;\theta_{oi},\phi_{oi}) = 4\pi \frac{I_{s\beta}(\theta_s,\phi_s)\cos\theta_s}{I_{oi\alpha}\cos\theta_{oi}}, \tag{10}$$

where $\alpha,\beta = v$ or h denoting vertical polarization or horizontal polarization, respectively. In the backscattering direction as $\theta_s = \theta_{oi}$ and $\phi_{os} = \pi + \phi_{oi}$, the backscattering cross section/unit area is defined as

$$\sigma^0_{\beta\alpha}(\theta_{oi}) = \cos\theta_{oi}\gamma_{\beta\alpha}(\theta_{oi},\pi + \phi_{oi};\theta_{oi},\phi_{oi}) = 4\pi\cos\theta_{oi}\frac{I_{oi\beta}(\theta_{oi},\pi + \phi_{oi})}{I_{oi\alpha}}. \tag{11}$$

The backscattering cross section/unit volume $\sigma_{\beta\alpha}$ is obtained by dividing $\sigma^0_{\beta\alpha}$ by the layer thickness d.

Another parameter that is of importance in the communications applications is the cross talk CX defined as the ratio of the power received through the offset channel to that through the direct channel. The total power in the line-of-sight direct channel is equal to the sum of the coherent and incoherent intensities

$$P_t = I_o \exp(-\kappa_e d\sec\theta_i) + \int_{\Omega_r} d\Omega' I_s(\pi - \theta',\phi') \approx I_o \exp(-\kappa_e d\sec\theta_i) + I_s(\pi - \theta_i,\phi_i,-d)\cdot\Omega_r. \tag{12}$$

The scattered power as received by the offset channel is

$$P_s = \int_{\Omega_r} d\Omega' I_s(\pi - \theta_s,\phi_s) \approx I_s(\pi - \theta_s,\phi_s,-d)\cdot\Omega_r, \tag{13}$$

where it is assumed that I_s is uniform over a very narrow radiant angle Ω_r of the antenna. The cross talk is defined as

$$CX = \frac{P_s}{P_t} = \frac{I_s(\pi - \theta_s,\phi_s,-d)\cdot\Omega_r}{I_o\exp(-\kappa_e d\sec\theta_i) + I_s(\pi - \theta_i,\phi_i,-d)\cdot\Omega_r}. \tag{14}$$

Notice that[11] $\Omega_r \approx \pi(\theta_{hr}/2)^2$ and $\theta_{hr} \approx \pi^2/G$ is the half-power beamwidth of the receiving antenna with gain G, where G is assumed to be 40 dB in our calculations.

IV. Iterative Approach

A. Iterative Procedure

When absorption is dominant over scattering, we can obtain closed-form solutions by using an iterative approach using the albedo (κ_s/κ_e) as the small parameter to carry out perturbation analysis. First, we break up the intensities in the scattering layer into backward propagating intensities $\bar{I}(\theta,\phi,z)$ and forward propagating intensities $\bar{I}(\pi - \theta,\phi,z)$ for $0 < \theta < \pi/2$. We then incorporate the boundary conditions to obtain the following integral equations:

$$\bar{I}(\theta,\phi,z) = \sec\theta\exp(-\kappa_e z\sec\theta)\int_{-d}^{z} dz' \exp(\kappa_e z'\sec\theta) \times \int_0^{\pi/2} d\theta' \sin\theta' \int_0^{2\pi} d\phi' \{\bar{\bar{P}}(\theta,\phi;\theta',\phi')\cdot\bar{I}(\theta',\phi',z') + \bar{\bar{P}}(\theta,\phi;\pi - \theta',\phi')\,\bar{I}(\pi - \theta',\phi',z')\}, \tag{15a}$$

$$\bar{I}(\pi - \theta,\phi,z) = \bar{I}_{oi}\delta(\cos\theta_o - \cos\theta_{oi})\delta(\phi_o - \phi_{oi})\exp(\kappa_e z\sec\theta) + \sec\theta\exp(\kappa_e z\sec\theta)\int_z^0 dz' \exp(-\kappa_e z'\sec\theta)\int_0^{\pi/2} d\theta' \sin\theta' \times \int_0^{2\pi} d\phi' \{\bar{\bar{P}}(\pi - \theta,\phi;\theta',\phi')\cdot\bar{I}(\theta',\phi',z') + \bar{\bar{P}}(\pi - \theta,\phi;\pi - \theta',\phi') \times \bar{I}(\pi - \theta',\phi',z')\}, \tag{15b}$$

where the first term of Eq. (15b) is the incident intensity in the θ_{oi},ϕ_{oi} direction. The zeroth-order solution takes the form

$$\bar{I}^{(0)}(\theta,\phi,z) = 0, \tag{16a}$$

$$\bar{I}^{(0)}(\pi - \theta,\phi,z) = \bar{I}_{oi}\delta(\cos\theta_o - \cos\theta_{oi}) \times \delta(\phi_o - \phi_{oi})\exp(\kappa_e z\sec\theta). \tag{16b}$$

The first-order solutions are found to be

$$\bar{I}^{(1)}(\theta,\phi,z) = \exp(-\kappa_e z\sec\theta)\sec\theta\bar{\bar{P}}(\theta,\phi;\pi - \theta_i,\phi_i)\cdot\bar{I}_{oi} \times \frac{\exp[\kappa_e z(\sec\theta + \sec\theta_i)] - \exp[-\kappa_e d(\sec\theta + \sec\theta_i)]}{\kappa_e(\sec\theta + \sec\theta_i)}, \tag{17a}$$

$$\bar{I}^{(1)}(\pi - \theta,\phi,z) = -\exp(\kappa_e z\sec\theta)\sec\theta\bar{\bar{P}}(\pi - \theta,\phi;\pi - \theta_i,\phi_i)\cdot\bar{I}_{oi} \times \frac{1 - \exp[-\kappa_e z(\sec\theta - \sec\theta_i)]}{\kappa_e(\sec\theta - \sec\theta_i)}. \tag{17b}$$

The corresponding first-order scattered intensities are, in region 0,

$$\bar{I}_o^{(1)}(\theta_{os},\phi_{os}) = \bar{I}^{(1)}(\theta_s,\phi_s,z = 0) = \sec\theta_s\bar{\bar{P}}(\theta_s,\phi_s;\pi - \theta_i,\phi_i) \times \bar{I}_{oi}\frac{1 - \exp[-\kappa_e d(\sec\theta_s + \sec\theta_i)]}{\kappa_e(\sec\theta_s + \sec\theta_i)} \tag{18a}$$

and in region 2

$$\bar{I}_2^{(1)}(\pi-\theta_{2s},\phi_{2s}) = \bar{I}^{(1)}(\pi-\theta_s,\phi_s,z=-d)$$
$$= -\exp(-\kappa_e d\sec\theta_s)\sec\theta_s$$
$$\bar{\bar{P}}(\pi-\theta_s,\phi_s,\pi-\theta_i,\phi_i)\cdot\bar{I}_{oi}$$
$$\cdot\frac{1-\exp[\kappa_e d(\sec\theta_s-\sec\theta_i)]}{\kappa_e(\sec\theta_s-\sec\theta_i)}. \tag{18b}$$

It is noted that, in the first-order solutions, the cross-polarization contributions are zero, and we must carry the iterative process to at least the second order to account for the depolarization effects.

The second-order solutions in region 0 in the direction $(\phi_{os},\pi+\phi_{os})$ are

$$\bar{I}_o^{(2)}(\theta_{os},\pi+\phi_{os}) = \sec\theta_s\int_0^{\pi/2}d\theta'\sin\theta'$$
$$\times\int_0^{2\pi}d\phi'\{\bar{\bar{P}}(\theta_s,\pi+\phi_s;\theta',\phi')$$
$$\times\bar{A}_1(\theta',\phi')+\bar{\bar{P}}(\theta_s,\pi+\phi_s;\pi-\theta',\phi')\cdot\bar{A}_2(\theta',\phi')\}, \tag{19a}$$

where

$$\bar{A}_1(\theta',\phi') = \int_{-d}^{0}dz'\exp(\kappa_e z'\sec\theta_i)\bar{I}^{(1)}(\theta',\phi',z')$$
$$= \sec\theta'\cdot\bar{\bar{P}}(\theta',\phi';\pi-\theta_i,\phi_i)\cdot\bar{I}_{oi}\cdot\frac{1}{\kappa_e(\sec\theta'+\sec\theta_i)}$$
$$\times\{D_2(\theta_s,\theta_i)-D_1(\theta_s,\theta')\exp[-\kappa_e d(\sec\theta'+\sec\theta_i)]\}, \tag{19b}$$

$$\bar{A}_2(\theta',\phi') = \int_{-d}^{0}dz'\exp(\kappa_e z'\sec\theta_i)\exp(\kappa_e z'\sec\theta')$$
$$\times\sec\theta'\cdot\bar{\bar{P}}(\pi-\theta',\phi';\pi-\theta_i,\phi_i)$$
$$\times\bar{I}_{oi}\cdot\frac{-1}{\kappa_e(\sec\theta'-\sec\theta_i)}\cdot\{1-\exp[-\kappa_e z'(\sec\theta'-\sec\theta_i)]\}$$
$$= \sec\theta'\cdot\bar{\bar{P}}(\pi-\theta',\phi';\pi-\theta_i,\phi_i)\cdot\bar{I}_{oi}\cdot\frac{-1}{\kappa_e(\sec\theta'-\sec\theta_i)}$$
$$\times[D_2(\theta_s,\theta')-D_2(\theta_s,\theta_i)], \tag{19c}$$

$$D_1(\theta_i,\theta_s) = \frac{1-\exp[-\kappa_e d(\sec\theta_i-\sec\theta_s)]}{\kappa_e(\sec\theta_i-\sec\theta_s)}, \tag{19d}$$

$$D_2(\theta_s,\theta_i) = \frac{1-\exp[-\kappa_e d(\sec\theta_s+\sec\theta_i)]}{\kappa_e(\sec\theta_s+\sec\theta_i)}. \tag{19e}$$

B. Backscattering and Bistatic Scattering Coefficients

We consider a vertically polarized incident wave and calculate the vertical and horizontal polarized scattered intensities to the second order in the iterative process. Using Eq. (19) we obtain

$$\bar{I}_{osv}^{(2)}(\theta_{os},\pi+\phi_{os}) = I_{oiv}\sec\theta_s\cdot\int_0^{\pi/2}d\theta'\sin\theta'\int_0^{2\pi}d\phi'\sec\theta'$$
$$\times\{[P_{11}(\theta_s,\pi+\phi_s;\theta',\phi')\cdot K_1(\theta',\phi')+P_{11}(\theta_s,\pi+\phi_s;\pi-\theta',\phi')$$
$$\times L_1(\theta',\phi')]+[P_{12}(\theta_s,\pi+\phi_s;\theta',\phi')\cdot K_2(\theta',\phi')$$
$$+P_{12}(\theta_s,\pi+\phi_s;\pi-\theta',\phi')\cdot L_2(\theta',\phi')]$$
$$+[P_{13}(\theta_s,\pi+\phi_s;\theta',\phi')\cdot K_3(\theta',\phi')+P_{13}(\theta_s,\pi+\phi_s;\pi-\theta',\phi')$$
$$\times L_3(\theta',\phi')]+[P_{14}(\theta_s,\pi+\phi_s;\theta',\phi')\cdot K_4(\theta',\phi')$$
$$+P_{14}(\theta_s,\pi+\phi_s;\pi-\theta',\phi')\cdot L_4(\theta',\phi')]\}. \tag{20}$$

where

$$K_1(\theta',\phi') = P_{11}(\theta',\phi';\pi-\theta_i,\phi_i)\frac{1}{\kappa_e(\sec\theta'+\sec\theta_i)}$$
$$\times\{D_2(\theta_s,\theta_i)-D_1(\theta_s,\theta')\exp[-\kappa_e d(\sec\theta'+\sec\theta_i)]\}, \tag{21a}$$

$$K_2(\theta',\phi') = P_{21}(\theta',\phi';\pi-\theta_i,\phi_i)\frac{1}{\kappa_e(\sec\theta'+\sec\theta_i)}$$
$$\times\{D_2(\theta_s,\theta_i)-D_1(\theta_s,\theta')\exp[-\kappa_e d(\sec\theta'+\sec\theta_i)]\}, \tag{21b}$$

$$K_3(\theta',\phi') = P_{31}(\theta',\phi';\pi-\theta_i,\phi_i)\frac{1}{\kappa_e(\sec\theta'+\sec\theta_i)}$$
$$\times\{D_2(\theta_s,\theta_i)-D_1(\theta_s,\theta')\exp[-\kappa_e d(\sec\theta'+\sec\theta_i)]\}, \tag{21c}$$

$$K_4(\theta',\phi') = P_{41}(\theta',\phi';\pi-\theta_i,\phi_i)\frac{1}{\kappa_e(\sec\theta'+\sec\theta_i)}$$
$$\times\{D_2(\theta_s,\theta_i)-D_1(\theta_s,\theta')\exp[-\kappa_e d(\sec\theta'+\sec\theta_i)]\}, \tag{21d}$$

$$L_1(\theta',\phi') = P_{11}(\pi-\theta',\phi';\pi-\theta_i,\phi_i)\cdot\frac{-1}{\kappa_e(\sec\theta'-\sec\theta_i)}$$
$$\times[D_2(\theta_s,\theta')-D_2(\theta_s,\theta_i)], \tag{22a}$$

$$L_2(\theta',\phi') = P_{21}(\pi-\theta',\phi';\pi-\theta_i,\phi_i)\cdot\frac{-1}{\kappa_e(\sec\theta'-\sec\theta_i)}$$
$$\times[D_2(\theta_s,\theta')-D_2(\theta_s,\theta_i)], \tag{22b}$$

$$L_3(\theta',\phi') = P_{31}(\pi-\theta',\phi';\pi-\theta_i,\phi_i)\cdot\frac{-1}{\kappa_e(\sec\theta'-\sec\theta_i)}$$
$$\times[D_2(\theta_s,\theta')-D_2(\theta_s,\theta_i)], \tag{22c}$$

$$L_4(\theta',\phi') = P_{41}(\pi-\theta',\phi';\pi-\theta_i,\phi_i)\cdot\frac{-1}{\kappa_e(\sec\theta'-\sec\theta_i)}$$
$$\times[D_2(\theta_s,\theta')-D_2(\theta_s,\theta_i)]. \tag{22d}$$

$P_{ij}(\theta,\phi,\theta',\phi')$ is the term of $\bar{\bar{P}}(\theta,\phi;\theta',\phi')$ $(i,j=1,2,3,4)$. Its expressions are given in Appendix A. Note that as $\theta'\to\theta_i$,

$$\lim_{\theta'\to\theta_i}\frac{-1}{\kappa_e(\sec\theta'-\sec\theta_i)}[D_2(\theta_s,\theta')-D_2(\theta_s,\theta_i)] = \frac{1}{\kappa_e(\sec\theta_s+\sec\theta_i)}$$
$$\times\{D_2(\theta_s,\theta_i)-D_1(\theta_s,\theta_i)\cdot\exp[-\kappa_e d(\sec\theta_s+\sec\theta_i)]\}. \tag{23}$$

Thus we can obtain the backscattering cross section

$$\sigma_{vv} = 4\pi\cos\theta_{oi}\frac{I_{osv}^{(1)}(\theta_i,\pi+\phi_i)+I_{osv}^{(2)}(\theta_i,\pi+\phi_i)}{I_{oiv}}, \tag{24}$$

and we can obtain the horizontal polarized scattered intensities

$$\bar{I}_{osh}^{(2)}(\theta_{os},\pi+\phi_{os}) = I_{oiv}\sec\theta_s\cdot\int_0^{\pi/2}d\theta'\sin\theta'\int_0^{2\pi}d\phi'\sec\theta'$$
$$\times\{[P_{21}(\theta_s,\pi+\phi_s;\theta',\phi')\cdot K_1(\theta',\phi')+P_{21}(\theta_s,\pi+\phi_s;\pi-\theta',\phi')$$
$$\times L_1(\theta',\phi')]+[P_{22}(\theta_s,\pi+\phi_s;\theta',\phi')\cdot K_2(\theta',\phi')$$
$$+P_{22}(\theta_s,\pi+\phi_s;\pi-\theta',\phi')\cdot L_2(\theta',\phi')]$$
$$+[P_{23}(\theta_s,\pi+\phi_s;\theta',\phi')\cdot K_3(\theta',\phi')+P_{23}(\theta_s,\pi+\phi_s;\pi-\theta',\phi')$$
$$\times L_3(\theta',\phi')]+[P_{24}(\theta_s,\pi+\phi_s;\theta',\phi')\cdot K_4(\theta',\phi')$$
$$+P_{24}(\theta_s,\pi+\phi_s;\pi-\theta',\phi')\cdot L_4(\theta',\phi')]\}. \tag{25}$$

Thus the bistatic scattering coefficient $\gamma_{ohv}(\theta_{os},\pi+\phi_{os};\theta_{oi},\phi_{oi})$ in region 0 is

$$\gamma_{ohv}(\theta_{os}\phi_{os};\theta_{oi},\phi_{oi}) = 4\pi\frac{\cos\theta_s I_{osh}(\theta_s,\phi_s)}{\cos\theta_{oi}I_{oiv}}$$
$$= 4\pi\sec\theta_s\cdot P_{21}(\theta_s,\pi+\phi_s;\pi-\theta_i,\phi_i)\cdot D_2(\theta_s,\theta_i)$$
$$+4\pi\sec\theta_s\int_0^{\pi/2}d\theta'\sin\theta'\sec\theta'\cdot[F_1(\theta_s,\theta')+F_2(\theta_s,\theta')$$
$$+F_3(\theta_s,\theta')+F_4(\theta_s,\theta')], \tag{26}$$

where

$$F_1(\theta_s,\theta') = \int_0^{2\pi} d\theta' [P_{21}(\theta_s,\pi+\phi_s;\theta',\phi')K_1(\theta',\phi') + P_{21}(\theta_s,\pi+\phi_s;\pi-\theta',\phi')L_1(\theta',\phi')]. \quad (27a)$$

$$F_2(\theta_s,\theta') = \int_0^{2\pi} d\theta' [P_{22}(\theta_s,\pi+\phi_s;\theta',\phi')K_1(\theta',\phi') + P_{22}(\theta_s,\pi+\phi_s;\pi-\theta',\phi')L_1(\theta',\phi')]. \quad (27b)$$

$$F_3(\theta_s,\theta') = \int_0^{2\pi} d\theta' [P_{23}(\theta_s,\pi+\phi_s;\theta',\phi')K_1(\theta',\phi') + P_{23}(\theta_s,\pi+\phi_s;\pi-\theta',\phi')L_1(\theta',\phi')]. \quad (27c)$$

$$F_4(\theta_s,\theta') = \int_0^{2\pi} d\theta' [P_{24}(\theta_s,\pi+\phi_s;\theta',\phi')K_1(\theta',\phi') + P_{24}(\theta_s,\pi+\phi_s;\pi-\theta',\phi')L_1(\theta',\phi')]. \quad (27d)$$

Using the similar approaches we can obtain $\sigma_{hh},\sigma_{hv},\sigma_{vh}$ in region 0. The second-order bistatic scattered intensity in region 2 in the $\pi-\theta_{2s},\phi_{2s}$ direction is

$$\begin{aligned}\bar{I}_2^{(2)}(\pi-\theta_{2s},\phi_{2s}) &= \bar{I}^{(2)}(\pi-\theta_s,\phi_s,z=-d)\\ &= \sec\theta_s \exp(-\kappa_e d\sec\theta_s)\\ &\times \int_{-d}^{0} dz' \exp(-\kappa_e z'\sec\theta_s) \int_0^{\pi/2} d\theta' \sin\theta' \int_0^{2\pi} d\phi'\\ &\times \{\bar{\bar{P}}(\pi-\theta_s,\phi_s;\theta',\phi')\cdot\bar{I}^{(1)}(\theta',\phi',z') + \bar{\bar{P}}(\pi-\theta_s,\phi_s;\pi-\theta',\phi')\\ &\times \bar{I}^{(1)}(\pi-\theta',\phi',z')\} = \sec\theta_s \exp(-\kappa_e d\sec\theta_s)\\ &\times \int_0^{\pi/2} d\theta' \sin\theta' \int_0^{2\pi} d\phi'\\ &\times \{\bar{\bar{P}}(\pi-\theta_s,\phi_s;\theta',\phi')\cdot\bar{B}_1(\theta',\phi') + \bar{\bar{P}}(\pi-\theta_s,\phi_s;\pi-\theta',\phi')\\ &\times \bar{B}_2(\theta',\phi')\}, \end{aligned} \quad (28)$$

where

$$\begin{aligned}\bar{B}_1(\theta',\phi') &= \int_{-d}^{0} dz' \exp(-\kappa_e z'\sec\theta_s)\bar{I}^{(1)}(\theta',\phi',z')\\ &= \sec\theta'\cdot\bar{\bar{P}}(\theta',\phi';\pi-\theta_i,\phi_i)\cdot\bar{I}_{oi}\cdot\frac{1}{\kappa_e(\sec\theta'+\sec\theta_i)}\\ &\times\left\{D_1(\theta_i,\theta_s) - \frac{\exp[-\kappa_e d(\sec\theta_i-\sec\theta_s)] - \exp[-\kappa_e d(\sec\theta'+\sec\theta_i)]}{\kappa_e(\sec\theta_s+\sec\theta')}\right\}, \end{aligned} \quad (29a)$$

$$\begin{aligned}\bar{B}_2(\theta',\phi') &= \int_{-d}^{0} dz' \exp(-\kappa_e d'\sec\theta_s)\cdot\bar{I}^{(1)}(\pi-\theta',\phi',z')\\ &= \sec\theta'\cdot\bar{\bar{P}}(\pi-\theta',\phi';\pi-\theta_i,\phi_i)\cdot\bar{I}_{oi}\cdot\frac{1}{\kappa_e(\sec\theta'-\sec\theta_i)}\\ &\times[D_1(\theta_i,\theta_s) - D_1(\theta',\theta_s)]. \end{aligned} \quad (29b)$$

C. Cross-Polarized Scattered Intensities

We consider a vertically polarized incident wave and calculate the scattered (i.e., incoherent) intensities (vertical co-polarized and horizontally depolarized scattered intensities) to the second order in the iterative process. Using Eqs. (28) and (29) we obtain co-polarized scattered intensity

$$\begin{aligned}I_{2sv}(\pi-\theta_{2s},\phi_{2s}) &= I_{2sv}^{(1)}(\pi-\theta_{2s},\phi_{2s}) + I_{2sv}^{(2)}(\pi-\theta_{2s},\phi_{2s})\\ &= \sec\theta_s\cdot\exp(-\kappa_e d\sec\theta_s)\cdot P_{11}(\pi-\theta_s,\phi_s;\pi-\theta_i,\phi_i)\cdot I_{oiv}\\ &\times D_1(\theta_i,\theta_s) + I_{oiv}\sec\theta_s\cdot\exp(-\kappa_e d\sec\theta_s)\\ &\times \int_0^{\pi/2} d\theta' \sin\theta' \int_0^{2\pi} d\phi'\\ &= \sec\theta'\{[P_{11}(\pi-\theta_s,\phi_s;\theta',\phi')\cdot R_1(\theta',\phi')\\ &+ P_{11}(\pi-\theta_s,\phi_s;\pi-\theta',\phi')\\ &\times S_1(\theta',\phi')] + [P_{12}(\pi-\theta_s,\phi_s;\theta',\phi')\cdot R_2(\theta',\phi')\\ &+ P_{12}(\pi-\theta_s,\phi_s;\pi-\theta',\phi')\cdot S_2(\theta',\phi')]\\ &+ [P_{13}(\pi-\theta_s,\phi_s;\theta',\phi')\cdot R_3(\theta',\phi') + P_{13}(\pi-\theta_s,\phi_s;\pi-\theta',\phi')\\ &\times S_3(\theta',\phi')] + [P_{14}(\pi-\theta_s,\phi_s;\theta',\phi')\cdot R_4(\theta',\phi')\\ &+ P_{14}(\pi-\theta_s,\phi_s;\pi-\theta',\phi')\cdot S_4(\theta',\phi')]\} \end{aligned} \quad (30)$$

and cross-polarized scattered intensity

$$\begin{aligned}I_{2sh}(\pi-\theta_{2s},\phi_{2s}) &= I_{2sh}^{(1)}(\pi-\theta_{2s},\phi_{2s}) + I_{2sh}^{(2)}(\pi-\theta_{2s},\phi_{2s})\\ &= \sec\theta_s\cdot\exp(-\kappa_e d\sec\theta_s)\cdot P_{21}(\pi-\theta_s,\phi_s;\pi-\theta_i,\phi_i)\cdot I_{oiv}\cdot D_1(\theta_i,\theta_s)\\ &+ I_{oiv}\sec\theta_s\cdot\exp(-\kappa_e d\sec\theta_s)\int_0^{\pi/2} d\theta'\sin\theta'\int_0^{2\pi} d\phi'\sec\theta'\\ &\times\{[P_{21}(\pi-\theta_s,\phi_s;\theta',\phi')\cdot R_1(\theta',\phi') + P_{21}(\pi-\theta_s,\phi_s;\pi-\theta',\phi')\\ &\times S_1(\theta',\phi')] + [P_{22}(\pi-\theta_s,\phi_s;\theta',\phi')\cdot R_2(\theta',\phi')\\ &+ P_{22}(\pi-\theta_s,\phi_s;\pi-\theta',\phi')\cdot S_2(\theta',\phi')]\\ &+ [P_{23}(\pi-\theta_s,\phi_s;\theta',\phi')\cdot R_3(\theta',\phi')\\ &+ P_{23}(\pi-\theta_s,\phi_s;\pi-\theta',\phi')\cdot S_3(\theta',\phi')] + [P_{24}(\pi-\theta_s,\phi_s;\theta',\phi')\\ &\times R_4(\theta',\phi') + P_{24}(\pi-\theta_s,\phi_s;\pi-\theta',\phi')\cdot S_4(\theta',\phi')]\}, \end{aligned} \quad (31)$$

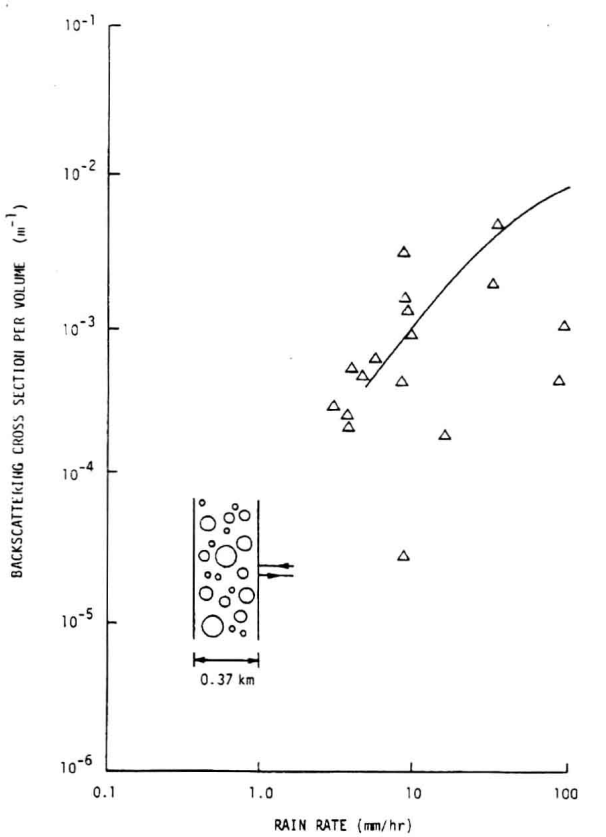

Fig. 4. Backscattering cross section/volume vs rain rate at 70 GHz. Data given in Ref. 5.

$$R_1(\theta',\phi') = P_{11}(\theta',\phi';\pi-\theta_i,\phi_i)\frac{1}{\kappa_e(\sec\theta'+\sec\theta_i)} \times\left\{D_1(\theta_i,\theta_s)-\frac{\exp[-\kappa_e d(\sec\theta_i-\sec\theta_s)]-\exp[-\kappa_e d(\sec\theta'+\sec\theta_i)]}{\kappa_e(\sec\theta_s+\sec\theta')}\right\}, \tag{32a}$$

$$R_2(\theta',\phi') = P_{21}(\theta',\phi';\pi-\theta_i,\phi_i)\frac{1}{\kappa_e(\sec\theta'+\sec\theta_i)} \times\left\{D_1(\theta_i,\theta_s)-\frac{\exp[-\kappa_e d(\sec\theta_i-\sec\theta_s)]-\exp[-\kappa_e d(\sec\theta'+\sec\theta_i)]}{\kappa_e(\sec\theta_s+\sec\theta')}\right\}, \tag{32b}$$

$$R_3(\theta',\phi') = P_{31}(\theta',\phi';\pi-\theta_i,\phi_i)\frac{1}{\kappa_e(\sec\theta'+\sec\theta_i)} \times\left\{D_1(\theta_i,\theta_s)-\frac{\exp[-\kappa_e d(\sec\theta_i-\sec\theta_s)]-\exp[-\kappa_e d(\sec\theta'+\sec\theta_i)]}{\kappa_e(\sec\theta_s+\sec\theta')}\right\}, \tag{32c}$$

$$R_4(\theta',\phi') = P_{41}(\theta',\phi';\pi-\theta_i,\phi_i)\frac{1}{\kappa_e(\sec\theta'+\sec\theta_i)} \times\left\{D_1(\theta_i,\theta_s)-\frac{\exp[-\kappa_e d(\sec\theta_i-\sec\theta_s)]-\exp[-\kappa_e d(\sec\theta'+\sec\theta_i)]}{\kappa_e(\sec\theta_s+\sec\theta')}\right\}, \tag{32d}$$

$$S_1(\theta',\phi') = P_{11}(\pi-\theta',\phi';\pi-\theta_i,\phi_i)\cdot\frac{1}{\kappa_e(\sec\theta'-\sec\theta_i)} \times[D_1(\theta_i,\theta_s)-D_1(\theta',\theta_s)], \tag{33a}$$

$$S_2(\theta',\phi') = P_{21}(\pi-\theta',\phi';\pi-\theta_i,\phi_i)\cdot\frac{1}{\kappa_e(\sec\theta'-\sec\theta_i)} \times[D_1(\theta_i,\theta_s)-D_1(\theta',\theta_s)], \tag{33b}$$

$$S_3(\theta',\phi') = P_{31}(\pi-\theta',\phi';\pi-\theta_i,\phi_i)\cdot\frac{1}{\kappa_e(\sec\theta'-\sec\theta_i)} \times[D_1(\theta_i,\theta_s)-D_1(\theta',\theta_s)], \tag{33c}$$

$$S_4(\theta',\phi') = P_{41}(\pi-\theta',\phi';\pi-\theta_i,\phi_i)\cdot\frac{1}{\kappa_e(\sec\theta'-\sec\theta_i)} \times[D_1(\theta_i,\theta_s)-D_1(\theta',\theta_s)]. \tag{33d}$$

Note that, as $\theta' \to \theta_i$,

$$\lim_{\theta'\to\theta_i}\frac{1}{\kappa_e(\sec\theta'-\sec\theta_i)}[D_1(\theta_i,\theta_s)-D_1(\theta',\theta_i)]=\frac{1}{2}d^2. \tag{34}$$

Thus by Eq. (14) we obtain the cross talk of a transmitting wave with vertical polarization:

$$CX=\frac{I_{2sv}(\pi-\theta_s,\phi_s,-d)\cdot\Omega_r}{I_{0v}\exp(-\kappa_e d\sec\theta_i)+I_{2sv}(\pi-\theta_i,\phi_i-d)\cdot\Omega_r} \tag{35}$$

$$=\frac{\cos\theta_i}{\cos\theta_s}\exp[-\kappa_e d(\sec\theta_s-\sec\theta_i)]\frac{[D_1(\theta_i,\theta_s)\cdot P_{11}^s+VV^s]\cdot\Omega_r}{\cos\theta_i+[d\cdot P_{11}^i+VV^i]\cdot\Omega_r},$$

where

$$P_{11}^l=P_{11}(\pi-\theta_l,\phi_l;\pi-\theta_i,\phi_i), \tag{36}$$

$$VV^l=\int_0^{\pi/2}d\theta'\sin\theta'\sec\theta'\{V_1(\theta_l,\theta')+V_2(\theta_l,\theta')+V_3(\theta_l,\theta')+V_4(\theta_l,\theta')\}, \tag{37}$$

where $l = i$ or s

$$V_1(\theta_l,\theta')=\int_0^{2\pi}d\theta'[P_{11}(\pi-\theta_l,\phi_l;\theta',\phi')\cdot R_1(\theta',\phi')+P_{11}(\pi-\theta_l,\phi_l;\pi-\theta',\phi')\cdot S_1(\theta',\phi')], \tag{38a}$$

$$V_2(\theta_l,\theta')=\int_0^{2\pi}d\phi'[P_{12}(\pi-\theta_l,\phi_l;\theta',\phi')\cdot R_2(\theta',\phi')+P_{12}(\pi-\theta_l,\phi_l;\pi-\theta',\phi')\cdot S_2(\theta',\phi')], \tag{38b}$$

$$V_3(\theta_l,\theta')=\int_0^{2\pi}d\theta'[P_{13}(\pi-\theta_l,\phi_l;\theta',\phi')\cdot R_3(\theta',\phi')+P_{13}(\pi-\theta_l,\phi_l;\pi-\theta',\phi')\cdot S_3(\theta',\phi')], \tag{38c}$$

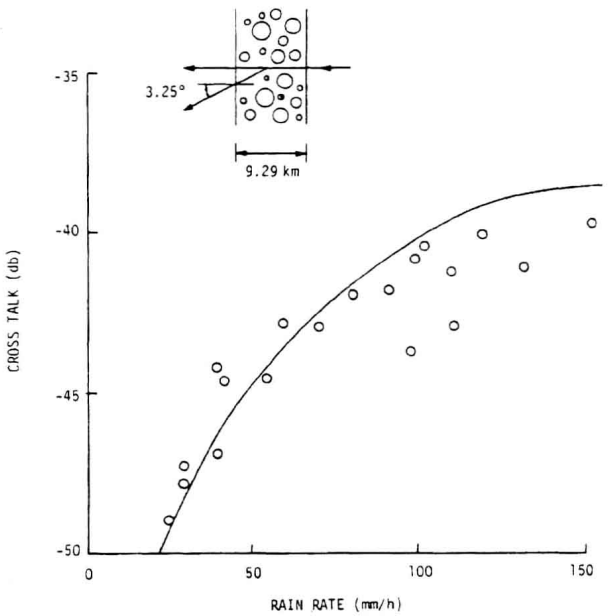

Fig. 5. Cross talk vs rain rate at 11 GHz. Data given in Ref. 8.